Chapter 6

Shear instabilities

In this final Chapter, we continue our study of the stability of fluid flows by looking at another very common source of instability, *shear*. By definition, shear occurs whenever two adjacent fluid parcels move in parallel directions, but at different velocities. The shear is defined as the amplitude of the local velocity gradient perpendicular to the motion.

Shear flows are *ubiquitous* in nature and can occur on any scale. Flows pumped though pipes by some pressure gradient along the pipe (called *Poiseuille flows*) are present everywhere in natural or engineered systems: blood flow through the body, from small capillaries to arteries, fluid flow through underground river systems, magma flows and pyroclastic flows through volcano chimneys, water flowing through a hose, a kitchen faucet, oil in a car engine, in a pipeline, etc.. These are often subject to strong shear if the wall boundaries are no-slip (so fluid is moving in the center of the pipe, but not on the sides. Shear flows can also be driven by differential pressure gradients (or any other forces) in open systems, and are found in the ocean, in the atmospheric wind patterns, in the surface and subsurface flows of the Sun, giant planets, other stars, in the orbital motion of gas in accretion disks, etc..

In this Chapter, we will apply some of the techniques learned in the context of convection to shear instabilities, and we will also see some new techniques. We will begin by looking at unstratified shear flows, and then move on to the more complicated problem of stratified shear flows.

6.1 Energetics of shear instabilities

The reason why shear drives instabilities is most easily understood by considering the energetics of a sheared fluid. The technique introduced here is actually widely applicable to many fluid instabilities, but it is worth bearing in mind that it is not very rigorous (nor is it meant to be), by contrast with all the other techniques introduced in the previous chapter.

Energetic considerations for the development of instabilities are based on

the following idea: given a background fluid flow, is that background the lowest possible energy state of the system, or can energy be *extracted* from the background by mixing material around? If it can, then instabilities are indeed energetically favorable because a perturbation can use the energy extracted from the background to amplify itself, in a positive feedback loop. This idea is illustrated below, for unstratified shear flows (see later for the case of stratified shear flows.)

Consider a simple background fluid flow, with constant density ρ_0, subject to some shear. Without loss of generality, the shear can be modeled locally as

$$\bar{\boldsymbol{u}} = \bar{u}(z)\boldsymbol{e}_x = \bar{u}(0) + Sz\boldsymbol{e}_x \tag{6.1}$$

where S is the (constant) shearing rate, by moving into a suitable frame of reference. This expression can, for instance, be viewed as a Taylor-expansion of the actual shear flow near a certain point.

Consider two parcels of fluid, one at $z = 0$, and one at $z = \epsilon$, where ϵ is small enough for (6.1) to be a good representation of the local flow. The initial total kinetic energy contained in the two parcels is

$$E_i = \frac{\rho_0}{2}\bar{u}(0)^2 + \frac{\rho_0}{2}\bar{u}(\epsilon)^2 = \frac{\rho_0}{2}\bar{u}(0)^2 + \frac{\rho_0}{2}\left(\bar{u}(0) + S\epsilon\right)^2 = \rho_0\bar{u}(0)^2 + \rho_0\bar{u}(0)S\epsilon + \frac{\rho_0}{2}S^2\epsilon^2 \tag{6.2}$$

Meanwhile, the momentum of the lower parcel is $\rho_0\bar{u}(0)$ while that of the upper parcel is $\rho_0\bar{u}(\epsilon) = \rho_0(\bar{u}(0) + S\epsilon)$.

Next, suppose we switch the two parcels around, but in the process, mix and equalize their momenta. If the total momentum remains conserved in the process, then the momenta of each of the two switched parcels becomes $\rho_0(\bar{u}(0) + S\epsilon/2)$, and they are both moving at the average velocity $\bar{u}(0) + S\epsilon/2$ (as shown in Figure 6.1). The total kinetic energy of the switched parcels is then

$$E_s = 2\frac{\rho_0}{2}\left(\bar{u}(0) + S\epsilon/2\right)^2 = \rho_0\bar{u}(0)^2 + 2\rho_0\bar{u}(0)S\epsilon + \frac{\rho_0}{4}S^2\epsilon^2 \tag{6.3}$$

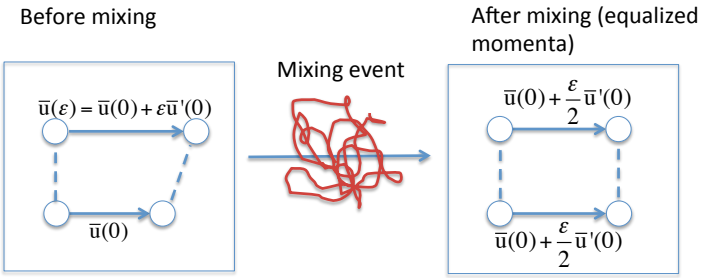

Figure 6.1: The mixing even equalizes the momenta of the two parcels of fluid.

We see that the new background flow consisting of the switched parcels has a lower energy than the original one. The difference

$$\Delta E = E_i - E_s = \rho_0 S^2\epsilon^2/4 > 0 \tag{6.4}$$

is available to amplify initial perturbations and thus drive instabilities. This is the main reason why shear instabilities are so common – the shear itself is a reservoir of kinetic energy that can, under some circumstances, be tapped into to drive instabilities.

6.2 Local linear stability analysis

As for the case of convection, we now attempt to perform a local stability analysis of shear flows. We do not need to specify the origin of the background shear, but merely assume it exists. We assume that the flow can be locally linearized, as in (6.1), with a constant shearing rate S. We also assume for simplicity that we are in the limit where the Boussinesq approximation is valid. If we let

$$\boldsymbol{u} = \bar{\boldsymbol{u}} + \tilde{\boldsymbol{u}} \tag{6.5}$$

then the perturbations evolve according to the linearized equation

$$\begin{aligned} &\nabla \cdot \tilde{\boldsymbol{u}} = 0 \\ &\frac{\partial \tilde{\boldsymbol{u}}}{\partial t} + \bar{\boldsymbol{u}} \cdot \nabla \tilde{\boldsymbol{u}} + \tilde{\boldsymbol{u}} \cdot \nabla \bar{\boldsymbol{u}} = -\frac{1}{\rho_0} \nabla \tilde{p} + \nu \nabla^2 \tilde{\boldsymbol{u}} \end{aligned} \tag{6.6}$$

Once expanded into components (and assuming 2D flow, for instance), this becomes

$$\begin{aligned} &\frac{\partial \tilde{u}}{\partial x} + \frac{\partial \tilde{w}}{\partial z} = 0 \\ &\frac{\partial \tilde{u}}{\partial t} + Sz\frac{\partial \tilde{u}}{\partial x} + S\tilde{w} = -\frac{1}{\rho_0}\frac{\partial \tilde{p}}{\partial x} + \nu \nabla^2 \tilde{u} \\ &\frac{\partial \tilde{w}}{\partial t} + Sz\frac{\partial \tilde{w}}{\partial x} = -\frac{1}{\rho_0}\frac{\partial \tilde{p}}{\partial z} + \nu \nabla^2 \tilde{w} \end{aligned} \tag{6.7}$$

We immediately detect a crucial problem: this equation does *not* have constant coefficients, so the standard *local* analysis (which would have us use the ansatz $\tilde{q} = \hat{q}\exp(ik_x x + ik_z z + \lambda t)$ will not work. However, for the specific case of linear shear flows, there is a nice trick we can play which involves moving into a *sheared* reference frame. Indeed, let

$$\begin{aligned} x' &= x - Szt \\ z' &= z \\ t' &= t \end{aligned} \tag{6.8}$$

then

$$\begin{aligned} \frac{\partial}{\partial x} &= \frac{\partial}{\partial x'} \\ \frac{\partial}{\partial z} &= \frac{\partial}{\partial z'} - St\frac{\partial}{\partial x'} \\ \frac{\partial}{\partial t} &= \frac{\partial}{\partial t'} - Sz\frac{\partial}{\partial x'} \end{aligned} \tag{6.9}$$

so the new equations are

$$\begin{aligned} \frac{\partial \tilde{u}}{\partial x'} + \frac{\partial \tilde{w}}{\partial z'} - St' \frac{\partial \tilde{w}}{\partial x'} &= 0 \\ \frac{\partial \tilde{u}}{\partial t'} + S\tilde{w} &= -\frac{1}{\rho_0}\frac{\partial p}{\partial x'} \\ \frac{\partial \tilde{w}}{\partial t'} &= -\frac{1}{\rho_0}\frac{\partial p}{\partial z'} + \frac{St'}{\rho_0}\frac{\partial p}{\partial x'} \end{aligned} \tag{6.10}$$

In this new coordinate system, there is no spatially-dependent coefficient, so we can indeed say that

$$\tilde{u} = \hat{u}(t') \exp(ik_x x' + ik_z z') \tag{6.11}$$

and similarly for the other variables. Then we have

$$\begin{aligned} ik_x \hat{u} + i(k_z - Sk_x t')\hat{w} &= 0 \\ \frac{d\hat{u}}{dt'} + S\hat{w} &= -\frac{i}{\rho_0} k_x \hat{p} \\ \frac{d\hat{w}}{dt'} &= -\frac{i}{\rho_0}(k_z - Sk_x t')\hat{p} \end{aligned} \tag{6.12}$$

Note, however, that if we wrote $\kappa_z(t') = k_z - Sk_x t'$ and $\kappa_x = k_x$ then

$$\begin{aligned} \kappa_x \hat{u} + \kappa_z(t')\hat{w} &= 0 \\ \frac{d\hat{u}}{dt'} + S\hat{w} &= -\frac{i}{\rho_0}\kappa_x \hat{p} \\ \frac{d\hat{w}}{dt'} &= -\frac{i}{\rho_0}\kappa_z(t')\hat{p} \end{aligned} \tag{6.13}$$

Now these look like they have time-independent coefficients, but they really don't since κ_z depends on t'.

Substituting one equation into the other, we eventually get (remembering that $t' = t$)

$$\frac{d\hat{w}}{dt} = \frac{\kappa_z(t)}{\kappa_x}\left[-\frac{\kappa_z(t)}{\kappa_x}\frac{d\hat{w}}{dt} + 2S\hat{w}\right] \tag{6.14}$$

which becomes the simple ODE for $\hat{w}$:

$$\left[1 + \frac{\kappa_z^2(t)}{\kappa_x^2}\right]\frac{d\hat{w}}{dt} = 2S\frac{\kappa_z(t)}{\kappa_x}\hat{w} \tag{6.15}$$

Since $d\kappa_z/dt = -Sk_x$, this can also be rewritten as

$$\frac{d}{dt}\left[\left(1 + \frac{\kappa_z^2(t)}{\kappa_x^2}\right)\hat{w}\right] = 0 \tag{6.16}$$

or, in other words,

$$\hat{w}(t) = \frac{C\kappa_x^2}{\kappa_x^2 + \kappa_z^2(t)} = \frac{Ck_x^2}{k_x^2 + (k_z - Sk_x t)^2} \tag{6.17}$$

where C is an arbitrary integration constant. As $t \to \infty$, $\hat{w}(t)$ always eventually tends to 0, which shows that the linear shear is always stable!

This result appears to contradict our energetic argument, which suggested that a non-viscous linear shear should be unstable. Is it really true? Or is it another one of these cases where the local analysis is giving weird results? The only way to find out is to abandon the local analysis and do the full problem in a bounded domain.

6.3 Global analysis of unstratified plane parallel flows

6.3.1 Linear stability analysis in the inviscid limit

We now consider a global model of fluid flow between two horizontal parallel plates, located at $z = 0$ and $z = H$. The plates are impermeable, so $w = 0$ on each plate. For simplicity, we assume again that there is no viscosity. In that case, we cannot apply any boundary conditions on u: the ones on w are sufficient to fully constrain the problem.

Let's first consider the background state. Interestingly, in the absence of viscosity, any shear flow in the x-direction, whose profile depends only on z but not on x or t (assuming a 2D system), is a solution of the steady-state momentum equation and of the continuity equation. In other words, the background flow $\bar{\boldsymbol{u}} = \bar{u}(z)\boldsymbol{e}_x$ satisfies

$$\begin{aligned} \frac{\partial \bar{\boldsymbol{u}}}{\partial t} + \bar{\boldsymbol{u}} \cdot \nabla \bar{\boldsymbol{u}} &= -\nabla \bar{p} \\ \nabla \cdot \bar{\boldsymbol{u}} &= 0 \end{aligned} \tag{6.18}$$

as long as $\nabla \bar{p} = 0$. Possible examples of such a background flow are shown in Figure 6.2.

Using the usual trick of setting $\boldsymbol{u} = \bar{\boldsymbol{u}} + \tilde{\boldsymbol{u}}$, and similarly for p, we can easily show that perturbations to this background flow satisfy

$$\begin{aligned} &\frac{\partial \tilde{u}}{\partial x} + \frac{\partial \tilde{w}}{\partial z} = 0 \\ &\frac{\partial \tilde{u}}{\partial t} + \bar{u}(z)\frac{\partial \tilde{u}}{\partial x} + \tilde{w}\frac{d\bar{u}}{dz} = -\frac{\partial \tilde{p}}{\partial x} \\ &\frac{\partial \tilde{w}}{\partial t} + \bar{u}(z)\frac{\partial \tilde{w}}{\partial x} = -\frac{\partial \tilde{p}}{\partial z} \end{aligned} \tag{6.19}$$

The coefficients of this system of PDEs are independent of time and of x, so we

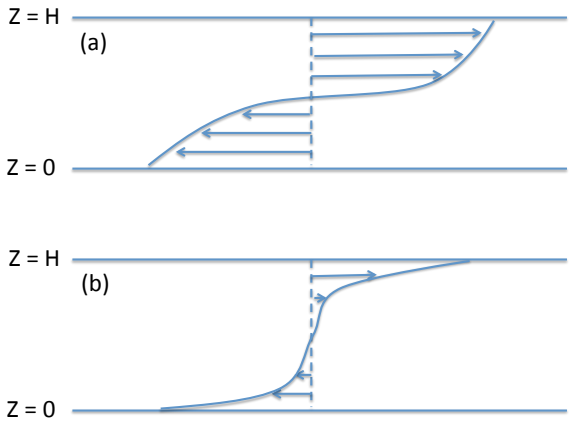

Figure 6.2: Illustration of possible background shear flows in a non-viscous system.

seek solutions of the form $\tilde{q}(x,z,t) = \hat{q}(z)\exp(ik_x x + \lambda t)$. We get

$$\begin{aligned} ik_x\hat{u} + \frac{d\hat{w}}{dz} &= 0 \\ \lambda\hat{u} + ik_x\bar{u}(z)\hat{u} + \hat{w}\frac{d\bar{u}}{dz} &= -ik_x\hat{p} \\ \lambda\hat{w} + ik_x\bar{u}(z)\hat{w} &= -\frac{d\hat{p}}{dz} \end{aligned} \tag{6.20}$$

Eliminating $\hat{p}$, we get

$$\left(\lambda + ik_x\bar{u}(z)\right)\frac{d\hat{u}}{dz} + \left(ik_x\hat{u} + \frac{d\hat{w}}{dz}\right)\frac{d\bar{u}}{dz} + \hat{w}\frac{d^2\bar{u}}{dz^2} = ik_x\left(\lambda + ik_x\bar{u}(z)\right)\hat{w} \tag{6.21}$$

We then use the continuity equation to eliminate $\hat{u}$, to get

$$\left(\lambda + ik_x\bar{u}(z)\right)\left(\frac{d^2\hat{w}}{dz^2} - k_x^2\hat{w}\right) - ik_x\hat{w}\frac{d^2\bar{u}}{dz^2} = 0 \tag{6.22}$$

Finally, if we define a new variable c such that

$$\lambda = -ik_x c \tag{6.23}$$

then the vertical velocity perturbation must satisfy

$$\left(\bar{u}(z) - c\right)\left(\frac{d^2\hat{w}}{dz^2} - k_x^2\hat{w}\right) - \hat{w}\frac{d^2\bar{u}}{dz^2} = 0 \tag{6.24}$$

where c is the eigenvalue of the problem.

This equation is called the *Rayleigh stability equation*. It is an ODE which needs to be solved for the function $\hat{w}(z)$ and the eigenvalue c, subject to the boundary conditions $\hat{w} = 0$ at the top and bottom of the domain. It usually needs to be solved numerically, and is not a standard Sturm-Liouville eigenvalue problem, so that most of the theorems we have learned about the latter do not apply here. Nevertheless, there are still an interesting number of strict results that can be derived from (6.24).

First, note that for any solution with $k_x > 0$, there is another solution with $k_x < 0$ (everything else being the same). Without loss of generality, we can therefore start by taking $k_x > 0$. Next, note that *unstable* modes for $k_x > 0$ are characterized by c values that have a positive imaginary part. Also it's easy to show that since $\hat{w}$ can be complex, if $\hat{w}$ is a solution then its complex conjugate $\hat{w}^*$ is also a solution with eigenvalue c^*. To see this, simply take the complex conjugate of the entire equation (6.24).

This means that there are only two possibilities: either the solution $\hat{w}$ has c real (the mode is called *neutrally stable* since it neither grows nor decays, but merely oscillates), or there is a complex-conjugate pair of solutions $\hat{w}$ and $\hat{w}^*$ with *one of the two being an unstable mode*. If c is real, then there is a possibility that the quantity $(\bar{u}(z) - c)$ could be zero somewhere in the domain. If this is the case, then the ODE is singular at this point. We shall return to that case later. For growing modes, however, c has a non-zero imaginary part, and the problem is regular everywhere.

Based on this consideration, we can then derive one of the most important results on plane parallel shear flows: *Rayleigh's inflection point theorem*. This theorem states that a necessary condition for the existence of a linearly unstable mode is that the flow profile must have an inflection point in the domain, that is, some point where $\bar{u}''(z) = d^2\bar{u}/dz^2 = 0$. To show this, first assume that c has a non-zero imaginary part, and rewrite (6.24) as

$$\frac{d^2\hat{w}}{dz^2} - k_x^2\hat{w} - \hat{w}\frac{\bar{u}''(z)}{\bar{u}(z) - c} = 0 \tag{6.25}$$

Then multiply this equation by $\hat{w}^*$, and integrate the result over z, from the bottom boundary (at $z = 0$) to the top boundary (at $z = H$). This yields

$$\int_0^H \left[\hat{w}^*\frac{d^2\hat{w}}{dz^2} - k_x^2|\hat{w}|^2 - |\hat{w}|^2\frac{\bar{u}''(z)}{\bar{u}(z) - c}\right] dz = 0 \tag{6.26}$$

The first term in the integral can then be integrated by parts, to give

$$\int_0^H \left[\left|\frac{d\hat{w}}{dz}\right|^2 + k_x^2|\hat{w}|^2 + |\hat{w}|^2\frac{\bar{u}''(z)}{\bar{u}(z) - c}\right] dz = 0 \tag{6.27}$$

The imaginary part of this equation is then

$$\Im(c)\int_0^H |\hat{w}|^2\frac{\bar{u}''(z)}{|\bar{u}(z) - c|^2}dz = 0 \tag{6.28}$$

Since all of the terms within the integral are strictly positive except $\bar{u}''(z)$, there are two possibilities: either $\bar{u}''(z)$ changes sign somewhere in the domain, or $\Im(c) = 0$ (which we had assumed is not the case). This shows that $\Im(c) \neq 0$ requires the presence of an inflection point! Note that the presence of an inflection point, by this analysis, is only a necessary condition for instability, but not a sufficient one, which means that there could be flows with an inflection point that are still stable. However, it does imply that flows without inflection point are always stable (in this inviscid limit).

Rayleigh's inflection point theorem has a really important, and rather peculiar consequence: it implies that linear shear flows (that is, flows of the kind described by (6.1)) are *linearly stable to shear instabilities*! This result is quite remarkable, and proves that the local analysis was right, in its stark contrast with our energetic argument, which suggested that linear shear flows in the inviscid limit should always be unstable. As it turns out, shear flows are quite different from the previously studied case of convection in that they are subject to finite amplitude instabilities, that is, they are often linearly stable, but can be destabilized by a strong enough perturbation. More on this later. In contrast, if the flow has an inflection point, then this is usually the position around which the shear instability will develop, and where the amplitude of the perturbation is the largest.

A number of additional interesting theorems can be derived from Rayleigh's instability equation. These include:

- *Fjortoft's theorem*: This is a stronger form of Rayleigh's inflection point criterion, which states that a necessary condition for instability is that $\bar{u}''(z)(\bar{u} - \bar{u}_i) < 0$ somewhere in the fluid, where $\bar{u}_i = \bar{u}(z_i)$ and where z_i is the point at which $\bar{u}''(z_i) = 0$. A more physical interpretation of Fjortoft's theorem is simply that the inflection point must correspond to a maximum in the shearing rate $S(z) = |du/dz|$ rather than a minimum. So for example (a) in Figure 6.2 could be linearly unstable, but (b) is not.

- *Howard's semicircle theorem*: This is a very useful theorem that bounds the possible values of the real and imaginary parts of c, and therefore places upper limits on the growth rate of the unstable modes. The theorem states that all unstable modes (that is with $\Im(c) > 0$) have an eigenvalue c that satisfies

$$\left(\Re(c) - \frac{\max\bar{u} + \min\bar{u}}{2}\right)^2 + \Im(c)^2 < \frac{(\max\bar{u} - \min\bar{u})^2}{2} \tag{6.29}$$

  or in other words, the complex number c lies on the complex plane within the semi-circle of radius $R = (\max\bar{u} - \min\bar{u})/4$, centered on the point $(\max\bar{u} + \min\bar{u})/2$ on the real axis.

The proof of these theorems can be found in the textbook *Hydrodynamic Stability* by Drazin and Reid, for instance, or in the original papers.

Finally, the combination of these theorems leads to the following strong statements (whose proofs are beyond the scope of this class). If $\bar{u}(z)$ is a smooth flow, then eigenmodes of Rayleigh's instability equation are of two kinds:

- Neutrally stable modes, with $\Im(c) = 0$. There is a continuum of them, one for each possible (real) value of c in the interval $[\min \bar{u}, \max \bar{u}]$. The modes are not defined at the point z where $\bar{u}(z) = c$, and their first derivative is discontinuous there. The position of this singularity is called a *critical layer*. Viscosity or nonlinearities can regularize the critical layer, but even with viscosity, many interesting phenomena can happen at a critical layer.
- Pairs of complex-conjugate modes, with $\Im(c) \neq 0$. There are only very few of them, at *most* one pair for each inflection point in the flow, and c for these complex-conjugate pairs satisfies Howard's semicircle theorem.

6.3.2 Examples of commonly-studied shear flows

Linear shear flows

As seen in the previous section, linear shear flows of the kind $\boldsymbol{u} = z\boldsymbol{e}_x$ are not expected to have any growing modes. Let's see this more directly by solving Rayleigh's instability equation subject to the boundary conditions $\hat{w} = 0$ at $z = -1$ and $z = 1$. Note how the velocity amplitude and domain height are now both non-dimensional. The equation simply becomes:

$$(z - c)\left(\frac{d^2\hat{w}}{dz^2} - k_x^2\hat{w}\right) = 0 \tag{6.30}$$

There are several possibilities:

- If c is real, and not in the interval $[-1, 1]$, then this can be rewritten as

  $$\frac{d^2\hat{w}}{dz^2} = k_x^2\hat{w} \tag{6.31}$$

  which has exponential solutions. However, these cannot be fitted to the homogeneous boundary conditions so this case is ruled out entirely.

- If c is complex, that is, $c = c_R + ic_I$ where $c_I \neq 0$, then (6.30) has a real and imaginary part, which are respectively:

  $$\begin{aligned}(z - c_R)\left(\frac{d^2\hat{w}_R}{dz^2} - k_x^2\hat{w}_R\right) + c_I\left(\frac{d^2\hat{w}_I}{dz^2} - k_x^2\hat{w}_I\right) = 0\\ (z - c_R)\left(\frac{d^2\hat{w}_I}{dz^2} - k_x^2\hat{w}_I\right) - c_I\left(\frac{d^2\hat{w}_R}{dz^2} - k_x^2\hat{w}_R\right) = 0\end{aligned} \tag{6.32}$$

  where $\hat{w} = \hat{w}_R + i\hat{w}_I$. These can be combined to get (for instance)

  $$\left[(z - c_R)^2 + c_I^2\right]\left(\frac{d^2\hat{w}_R}{dz^2} - k_x^2\hat{w}_R\right) = 0 \tag{6.33}$$

and similarly for $\hat{w}_I$. Since c_I was by assumption non-zero, we end up again with equation (6.31) whose exponential solutions cannot be fitted to the boundary conditions. This has a very important implication: remembering that $\lambda = -ik_x c$, we can only get growing solutions if c_I is non-zero – but we just ruled this possibility out. Hence, as expected, we find that there are no linearly unstable modes in linear shear flows.

- Finally, if c is real and lies within the interval $[-1, 1]$, then for any selected value of c, (6.30) is singular at the point $\bar{u}(z_s) = z_s = c$, and the derivative must be discontinuous at z_s. Solutions can be found by solving (6.30) on both sides of z_s, and matching them to one another at that point requiring continuity of $\hat{w}$.

  Solving (6.30) for $z > z_s$, and applying $\hat{w} = 0$ at $z = 1$, we get

$$\hat{w} = w_+ \sinh(k_x(z-1)) \tag{6.34}$$

  Similarly for $z < z_s$:

$$\hat{w} = w_- \sinh(k_x(z+1)) \tag{6.35}$$

  Matching the two at $z = c$, we have

$$w_+ \sinh(k_x(c-1)) = w_- \sinh(k_x(c+1)) \tag{6.36}$$

  This can be rewritten as

$$w_+ = \frac{w_0}{\sinh(k_x(c-1))} \text{ and } w_- = \frac{w_0}{\sinh(k_x(c+1))} \tag{6.37}$$

  where w_0 is the total mode amplitude, which remains arbitrary since this is a linear problem. So finally, for every value of c in the interval $[-1, 1]$, we get one eigenmode $\hat{w}(z)$ as:

$$\begin{aligned} \hat{w} &= \frac{w_0}{\sinh(k_x(c-1))} \sinh(k_x(z-1)) \text{ for } c \le z \le 1 \\ \hat{w} &= \frac{w_0}{\sinh(k_x(c+1))} \sinh(k_x(z+1)) \text{ for } -1 \le z \le c \end{aligned} \tag{6.38}$$

  A particular mode for $k_x = 1$, for $c = -0.2$ is shown in Figure 6.3. Note how $\hat{w}$ is continuous but its derivative isn't. This implies, by the continuity equation, that the horizontal flow velocity u is discontinuous. Of course, this can only happen in the non-viscous case (viscosity would otherwise tend to smooth-out the discontinuity, thereby disallowing this kind of solution). See more in the next section on the effect of viscosity on linear shear flows.

To summarize these results, we have seen that, as discussed in the previous section, a linear shear is linearly stable, but there is a continuum of neutral modes where the real part of c lies in between the minimum and the maximum of $\bar{u}(z)$. With $\lambda = -ik_x c$, the full solution for the vertical velocity is

$$w(x, z, t) = \Re\left(\hat{w}(z) e^{ik_x(x-ct)}\right) \tag{6.39}$$

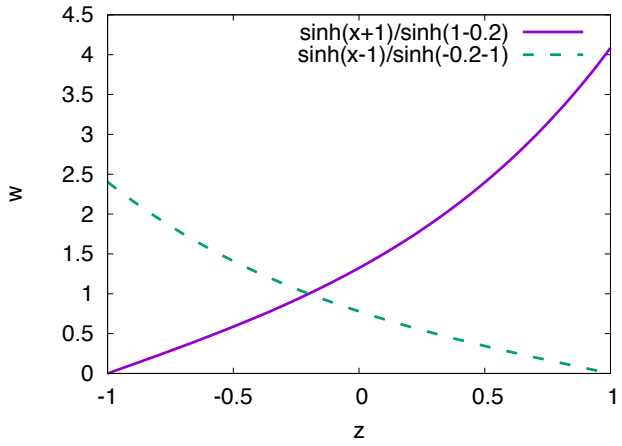

Figure 6.3: Vertical velocity profile for the neutral mode with $k_x = 1$, for $c = -0.2$

where $\hat{w}$ is given in equation (6.38). The neutral modes thus discovered are a form of oscillation propagating in the x-direction at velocity c without change of form.

The Bickley jet

There are not many continuous profiles $\bar{u}(z)$ for which analytical solutions of Rayleigh instability equation exist. In general, solutions and their corresponding eigenvalues have to be computed numerically. In the following example, which studies the *Bickley jet*, some of the solutions can be found analytically, and some must be found numerically.

The Bickley jet is of the form

$$\bar{u}(z) = \operatorname{sech}^2(z)\boldsymbol{e}_x = \frac{1}{\cosh^2(z)}\boldsymbol{e}_x \tag{6.40}$$

and is shown in Figure 6.4. The first and second derivatives are

$$\begin{aligned} \bar{u}'(z) &= -2\tanh(z)\bar{u}(z) \\ \bar{u}''(z) = -2\tanh(z)\bar{u}'(z) - 2\operatorname{sech}^2(z)\bar{u}(z) &= 2(2 - 3\bar{u}(z))\bar{u}(z) \end{aligned} \tag{6.41}$$

This has an inflection point at positions z_i such that $\bar{u}(z_i) = 2/3$ (which happens at two positions, one below 0 and one above 0). We therefore expect, for each value of k_x, at most 2 pairs of complex-conjugate modes. As it turns out, because of the symmetries of the jet, there are indeed 2 modes: one for which $\hat{w}$ is symmetric with respect to z (called the *sinuous mode*), and one for which $\hat{w}$ is antisymmetric with respect to z (called the *varicose mode*).

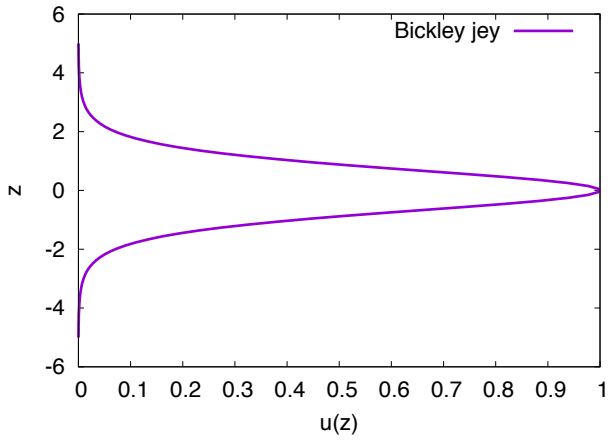

Figure 6.4: Bickley jet

To find growing modes, one needs to solve Rayleigh's instability equation numerically. As before, we first isolate the real and imaginary parts of this equation, to get:

$$\begin{aligned}(\bar{u}(z)-c_R)\left(\frac{d^2\hat{w}_R}{dz^2}-k_x^2\hat{w}_R\right)+c_I\left(\frac{d^2\hat{w}_I}{dz^2}-k_x^2\hat{w}_I\right)-\hat{w}_R\bar{u}''(z)=0\\(\bar{u}(z)-c_R)\left(\frac{d^2\hat{w}_I}{dz^2}-k_x^2\hat{w}_I\right)-c_I\left(\frac{d^2\hat{w}_R}{dz^2}-k_x^2\hat{w}_R\right)-\hat{w}_I\bar{u}''(z)=0\end{aligned} \tag{6.42}$$

We then reshuffle them as

$$\begin{aligned}\frac{d^2\hat{w}_R}{dz^2}-k_x^2\hat{w}_R-\frac{(\bar{u}(z)-c_R)\hat{w}_R-c_I\hat{w}_I}{(\bar{u}(z)-c_R)^2+c_I^2}\bar{u}''(z)=0\\\frac{d^2\hat{w}_I}{dz^2}-k_x^2\hat{w}_I-\frac{c_I\hat{w}_R+(\bar{u}(z)-c_R)\hat{w}_I}{(\bar{u}(z)-c_R)^2+c_I^2}\bar{u}''(z)=0\end{aligned} \tag{6.43}$$

We then solve these equations numerically, using for instance a Newton-Raphson two-point boundary value relaxation method. To find the sinuous and varicose modes, we limit the domain to $z>0$ and require that $d\hat{w}/dz=0$ at $z=0$ for the sinuous mode, and $\hat{w}=0$ at $z=0$ for the varicose mode. The figure below shows c_I as a function of k_x for the sinuous mode. We see that growing modes only exist for small enough k_x (that is, $k_x<2$), and that there is a most rapidly growing mode whose wavenumber is approximately $k_x=0.1$. For the varicose mode, the maximum wavenumber that is unstable is $k_x=1$, and the growth rate of the varicose modes are always smaller than those of the sinuous modes (see Figure 6.5).

Interestingly, the marginal modes (that is, the modes for which c_I is identi-

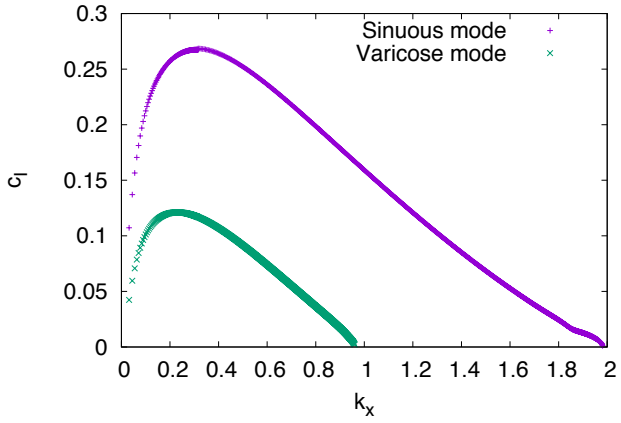

Figure 6.5: Imaginary part of c (which is proportional to the growth rate λ) for the sinuous and varicose modes.

cally zero) can be found analytically. It's easy to check that they have

$$\begin{aligned} k_x = 2 \ , \ c_R = \frac{2}{3} \ , \ \hat{w} = \mathrm{sech}^2(z) \text{ for the sinuous mode} \\ k_x = 1 \ , \ c_R = \frac{2}{3} \ , \ \hat{w} = \mathrm{sech}(z)\tanh(z) \text{ for the varicose mode} \end{aligned} \quad (6.44)$$

The fact that c_R is equal to value of $\bar{u}(z)$ at the inflection point, for these marginal modes, is not a coincidence. It it the only real value of c_R for which a *non-singular* solution to Rayleigh's equation can exist.

Finally, note that in addition to the regular marginal and growing modes, there is also a continuum of singular modes whose eigenvalue c is real, and lies between 0 and 1. These can be found, as before, by seeking solutions on either sides of the singular point, and matching them to one another, and to the boundary conditions at infinity.